The Binary Systems Sodium Sulfide–Sodium Hydroxide and Sodium Carbonate–Sodium Hydroxide

Premo Chiotti* and Richard Markuszewski

Ames Laboratory† and Department of Materials Science and Engineering, Iowa State University, Ames, Iowa 50011

The binary system Na_2S–NaOH was investigated by differential thermal analysis, and the room-temperature phases were determined by X-ray diffraction data. This system is a simple eutectic system. The eutectic temperature and composition are 296 ± 1 °C and 0.05 mole fraction Na_2S. The polymorphic transformation in NaOH occurred at 291 °C. The lowering of this transition from 293.1 °C, the accepted value, is believed to be due to residual moisture in the NaOH. No evidence for the two compounds Na_2S·NaOH and Na_2S·2NaOH, reported in the literature, was observed. Mixtures of these compositions gave thermal arrests at eutectic and transformation temperature. X-ray diffraction patterns showed lines which could be accounted for on the basis of known patterns for cubic Na_2S and orthorhombic NaOH. Literature data for the NaOH–Na_2CO_3 system were reviewed and employed to construct the phase diagram. This is also a simple eutectic system with a eutectic temperature and composition of 288 ± 1.0 °C and 92.0 ± 0.1 mol % NaOH.

Introduction

The Na_2S–NaOH and Na_2CO_3–NaOH systems are of interest in the chemical desulfurization of coal (*1*). The solubility of Na_2S in fused NaOH and possible compounds between these two components are of particular interest in the treatment of coal with fused alkali. A recent study (*2*) of the reaction of pyrite (FeS_2) with NaOH at 350 °C showed that Na_2S is one of the principal products of this reaction. No evidence was found for the two compounds Na_2S·NaOH and Na_2S·2NaOH reported (*3*) to exist in the system Na_2S–NaOH. Consequently a rather detailed investigation of this system was carried out by using thermal and X-ray diffraction analyses to determine the phases present. A review of the literature revealed sufficient data to permit construction of the Na_2CO_3–NaOH phase diagram.

Literature Review

The Na_2S–NaOH system has been investigated previously by Ovechkin et al. (*3*). They report the existence of two compounds, Na_2S·2NaOH, which undergoes a peritectic reaction at 675 °C, and Na_2S·NaOH, which melts congruently at 875 °C. Their NaOH was dried by fusion at 400–425 °C under vacuum. The melting temperature was found to be 324 ± 3 °C, and it underwent a polymorphic transition of 300 ± 3 °C. They dried Na_2S·$9H_2O$ by a final step at 700 °C under a stream of dried nitrogen. The product was a pale pink material which melted at 1160 °C. In an earlier investigation of the Na_2S–Na_2CO_3 system, Ovechkin and Shevtsova (*4*) report a polymorphic transition in Na_2S at 320 °C.

Kohlmayer and Lohrke (*5*) produced a brownish-red Na_2S. The molten product solidified on cooling at 1180 °C. Steck et al. (*6*) prepared Na_2S from Na_2S·$9H_2O$ in a vacuum desiccator at 150 °C with P_2O_5 desiccant. Their product analyzed 95% Na_2S and solidified on cooling from the melt at 970 °C. Kopylov and Novoselov (*7*) in their study of Na_2S–Cu_2S–FeS binary and ternary systems report a melting temperature of 1175 °C for Na_2S. The JANAF Tables (*8*) give 1225 K (950 °C) as the melting temperature of Na_2S. None of these investigators report a polymorphic transition for Na_2S.

Morey and Burlew (*9*) did a study of the freezing and polymorphic transition temperatures of NaOH as a function of Na_2O content. The starting NaOH contained 0.24 wt % CO_2 or 0.22 mol % Na_2CO_3. They obtained a melting point maximum of 318 °C at 77.37 wt % Na_2O. The theoretical value for pure anhydrous NaOH is 77.48 wt % Na_2O. Their correction for the presence of 0.22 mol % Na_2CO_3 yielded a melting temperature of 319.2 °C. They observed a polymorphic transition temperature of 293.1 °C which is lowered to 287.7 ± 3 °C as the Na_2O content is decreased or the H_2O content is increased. They also established the eutectic temperature and composition for the NaOH–Na_2CO_3 binary system as 287.9 ± 0.2 °C at 92.1 mol % NaOH. They apparently employed their data on the melting point lowering of NaOH by Na_2CO_3 to correct the above melting temperature of NaOH. Other data for this system have been summarized by Voskresenskaya (*10*).

The JANAF Tables (*8*) give 319.2 and 292.8 °C as the melting and transition temperatures of NaOH, respectively.

Materials

Analytical-grade NaOH was dried by heating it under vacuum at 300–310 °C for 4 h. The mechanical vacuum pump employed was capable of a pressure as low as 1×10^{-4} torr (0.013 Pa). Analysis of the dried product by potentiometric titration with HCl indicated 99.7 ± 0.1 mol % NaOH and 0.3 ± 0.1 mol % Na_2CO_3. Anhydrous Na_2S was prepared by heating Na_2S·$9H_2O$ under vacuum to 650–700 °C, held at this temperature for 4 h, and then furnace-cooled overnight. One 500-g sample contained in an Inconel crucible was slowly heated to 700 °C. No liquid phases occurred during this heating cycle. The product was a pure white, partially sintered powder. This material analyzed 97.0 wt % Na_2S by potentiometric titration with HCl. A second run with 500 g of Na_2S·$9H_2O$, heated to 700 °C more rapidly but otherwise treated the same, yielded a salt with a pinkish tint. A similar run with the salt in a 500-mL Pyrex beaker heated to 650 °C yielded a white salt. The white salts when added to distilled water yielded a colorless solution, whereas the slightly pink salt yielded a bluish-green solution. The blue-green color probably indicates slight contamination by the Inconel container. Addition of iron or nickel ions to a solution containing Na_2S produces a dark green, almost black precipitate and solution. Very low concentrations of iron or nickel produce a clear bluish-green solution. Samples of all three batches of salt gave X-ray diffraction patterns in good agreement with Powder Diffraction File (*11*) data, microfilm 23-441, for cubic Na_2S. The first salt described above was used in the preparation of NaOH–Na_2S mixtures, except for a few mixtures in the high-Na_2S region as noted below.

Experimental Section

All the dried salts were removed from the resistance furnace employed and placed in a desiccator. They were then trans-

† Ames Laboratory is operated for the U.S. Department of Energy by Iowa State University under Contract No. W-7405-Eng-82.

0021-9568/85/1730-0197$01.50/0

Table I. DTA Arrests for Na_2S–NaOH Mixtures

X_{Na_2S}	container[a]	cooling arrests, °C 1	2	3	4	remarks T_{max}, °C	cycles
0.00	SS	319		295		586	3
0.00	Ta	316		291		462	1
0.00	Ta	317		291	244	438	1
0.02	Ta	311	294	292		435	2
0.034	Ta		298	290		462	1
0.049	Ta		295	290	269	532	2
0.05	Ta		295	290	268	438	1
0.075	Ta	348	296	292		450	3
0.077	Ta	350	297	293	261	560	1
0.10	Ta	403	297	290		580	2
0.15	Ta	462	294	290	271	569	2
0.20	Ta	532	295	290	266	565	2
0.23	Ta	551	297	292	265	612	2
0.30	Ta		296	291		593	2
0.30	Ta	625	302		274	685	1
0.30	C	626	295	291	270	710	3
0.33	C	670	295	280	268	700	2
0.40	SS		296	291	259	711	2
0.40	SS	732	296	290	263	793	1
0.50	C	854	298	291		880	1
0.50	Ta		295	285	271	426	1
0.60	C		290	276	269	485	1

[a] SS = 18-8 stainless steel. Ta = tantalum. C = graphite.

ferred to a helium-filled glovebox. Exposure to the atmosphere was avoided as much as possible because both NaOH and Na_2S readily absorb CO_2 and particularly H_2O from the atmosphere. The helium atmosphere was kept dry by circulating it through Linde 13x molecular sieve. Periodically it was further purified by circulating it over zirconium shavings and titanium sponge at 650 °C.

The differential thermal analysis (DTA) apparatus employed is described in detail in an earlier publication (*12*). Tantalum capsules were suitable for temperatures below 650–700 °C. At higher temperatures, reaction between the salt and tantalum becomes significant. The tantalum capsules were 0.95 cm in diameter and 5.05 cm long with a tantalum thermocouple well 0.32 cm in diameter extending up through the bottom. The capsules were made from 0.010-in. (0.254-mm) tantalum tubing and were assembled by electron beam welding. For higher temperatures, capsules were machined from high-density graphite. However, because it was necessary to have a greater wall thickness, 2.4 mm, the amount of sample was restricted to about 0.5 g. Also very little or no salt surrounded the thermocouple well and the DTA sensitivity was greatly reduced. The maximum temperature for this DTA apparatus was 950 °C. A furnace with a 1.0 in. (2.54 cm) inside diameter graphite tube heating element surrounded by tantalum radiation shields was employed for higher temperatures. This furnace could be operated under vacuum or an inert atmosphere. Graphite crucibles with a capacity of 10.0 g of salt with a graphite thermocouple well inserted into the salt served satisfactorily for temperature–time plots up to 1300 °C. DTA plots were also obtained with this apparatus which were only moderately satisfactory.

Temperatures were measured with chromel–alumel thermocouples. With graphite capsules, penetration of the salt to the thermocouple well sometimes occurred, especially if recycled through temperatures above 800 °C. Occasional overflow of molten salt sometimes occurred on melting in tantalum capsules, apparently due to outgassing on fusion. In each case the thermocouple was replaced by a new couple made from the same spools of wire. Thermocouples made from these spools were checked against the melting temperature of high-purity zinc, magnesium, silver, and copper. The DTA apparatus reproduced the melting point of zinc, 419.5 °C, to ±0.5 °C and the melting point of magnesium, 649 °C, to ±1 °C. In earlier investigations this same apparatus was checked against the melting temperature of silver, 961 °C.

Table II. High-Temperature Thermal Data for Na_2S–NaOH Mixtures Heated in Graphite Crucibles

X_{Na_2S}	thermal breaks, °C heating	cooling	remarks
1.0	1215	1188	
	1218	1180	
1.0[a]	1212	1182	
		1188	
0.8	1062	1062	
0.65	931	929	av. of 3 cycles, 930 ± 3 °C
0.60		915	
0.50[b]	864		290, 276, 261 °C

[a] Salt with pink cast; see text. [b] No freezing break was discernible for this sample but three definite cooling breaks were detected near the eutectic and transition temperatures. Part of this sample was powdered and loaded into a tantalum capsule and run in the DTA apparatus to further define the low-temperature breaks. See the last two curves in Figure 1.

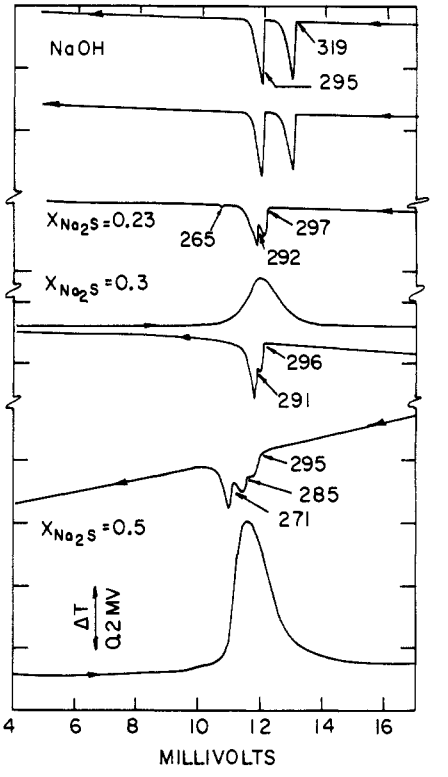

Figure 1. DTA arrests observed in the eutectic and transition temperature range. The scales in millivolts are for a chromel–alumel thermocouple and the indicated transition temperatures are in degrees Celsius.

The desired components were weighed and thoroughly mixed with a mortar and pestle in the helium glovebox. Capsules containing the salt were put into glass jars and transferred to the DTA apparatus or furnace. Similarly equilibrated salts were transferred to the glovebox, samples powdered and loaded into capillaries for Debye–Scherrer powder diffraction patterns. The camera was 114.6 mm in diameter. The capillaries were irradiated with nickel-filtered copper Kα radiation. The capillaries were sealed at both ends to exclude atmospheric moisture.

Thermal Results for Na_2S–NaOH Mixtures

Results of DTA and temperature–time analyses are summarized in Tables I and II. Of particular interest are the thermal arrests at the eutectic temperature, 296 °C, and the NaOH transition temperature, 291 °C, extending across the entire span of compositions investigated. Typical low-temperature

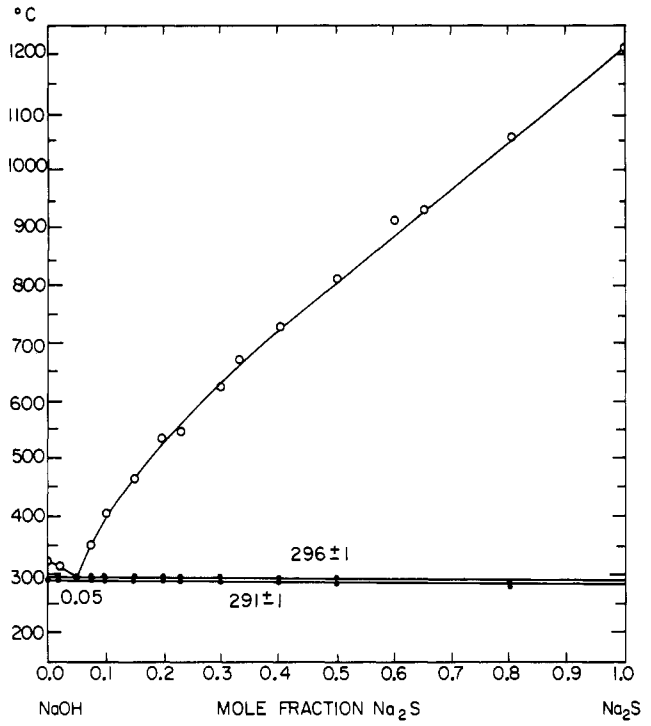

Figure 2. Binary Na_2S–NaOH phase diagram.

DTA curves are shown in Figure 1. The cooling arrests tabulated under 4 in Table I are rather anomolous. The arrest, once it appeared, was reproducible. It occurred over a temperature range of 244–270 °C and was usually very weak. See the cooling curve for the mixture with mole fraction X_{Na_2S} = 0.23 in Figure 1. However, in some samples the arrest was very pronounced (see the cooling curve for X_{Na_2S} = 0.5). It should be noted that in this case the sample was made up from material that had been melted in graphite. See the last sample listed in Table II. Here the temperature–time plot showed breaks at 290, 276, and 261 °C as compared with arrests at 295, 285, and 271 °C obtained in the DTA apparatus. The lower temperatures in the temperature–time breaks are believed to be due to supercooling because of a higher cooling rate. The cooling rate in the DTA apparatus varied between 10 to 6 °C/min. The initial heating rate in this apparatus was approximately 20 °C/min and as may be seen in Figure 1 only one pronounced peak was obtained for samples X_{Na_2S} = 0.5 and 0.3. The fine structure was not resolved on heating.

The low-temperature anomalous thermal arrest has been observed in experiments in the high-temperature apparatus and the low-temperature DTA apparatus and with different container materials. One possible explanation of two thermal arrests following the eutectic arrest is that the polymorphic transformation of NaOH occurs in two steps. It could first transform to a metastable crystalline state followed by a final transformation to the low-temperature stable state. Such a sequence could be dependent on the cooling rate. Time did not permit an investigation of this possibility.

The average of the eutectic arrests, cooling arrests column 2, Table I, is 295.8 °C and is indicated on the phase diagram (Figure 2) as 296 ± 1 °C. The polymorphic transition temperature for NaOH established by Morey and Burlew (*9*) is 293.1 °C. The average of cooling arrests, column 3, Table I, is 291.1 °C, excluding the 280 and 276 values. This is 2 °C lower than Morey and Burlew's value and is probably due to small amounts of residual water and Na_2CO_3 in the starting materials. The effect of water was corrected for by Morey and Burlew, who showed that water can lower the transition temperature of NaOH to 287.7 °C. In Figure 2 the transition temperature is indicated as 291 ± 1 °C.

The melting temperature for Na_2S was observed to be 1215 ± 3 °C average for two different batches of dried salt. See Table II. Both salts were run through two cycles. Cooling thermal arrests were observed for each sample with an average value of 1184.5 ± 4 °C. Because of the tendency of pure salts to supercool, the heating value of 1215 is considered to be nearer the true melting temperature. The heating and cooling rates through the fusion temperature were approximately 50 °C/min.

The salt heated above 1200 °C yielded a black crystalline solid with a bright shiny fracture. The sample with 0.8 mole fraction Na_2S heated to near 1100 °C yielded a white crystalline mass.

X-ray Diffraction Data for Na_2S–NaOH Samples

A portion of the black material obtained after heating Na_2S to above 1200 °C was ground to a fine powder and a Debye–Scherrer powder pattern taken. The indices (*hkl*) for the diffraction lines of Na_2S, which is face-centered cubic, are readily assigned and are listed in Table III. In the back-reflection region the lattice constant $a_0 = d(h^2 + k^2 + l^2)^{1/2}$ is a linear function of $\cos^2\theta$ where θ is the reflection angle. A least-squares treatment of a_0 as a function of $\cos^2\theta$ for $d < 1.45$ extrapolated to $\cos^2\theta = 0$ yielded a_0 = 0.6541 ± 0.002 nm. The literature data (*12*) for Na_2S (see Table III) given the same treatment yielded a_0 = 0.65395 ± 0.00016 nm. The two values are within the experimental error. Consequently, the black material is still relatively pure Na_2S with no significant change in lattice constant. The black color is possibly due to dissolution of carbon in Na_2S near 1200 °C. It was noted that when the black material was ground in a mortar, black streaks were formed on the bottom of the mortar and on the pestle, apparently due to carbon. The powder was no longer black but had a light purple to gray color. It should be noted that it is not impossible that the black material is not face-centered cubic but undergoes a stress induced transition on grinding it to a fine powder. No transition was observed in the dried Na_2S powder when run on the DTA apparatus to temperatures as high as 700 °C.

Special attention was also given to the compositions corresponding to Na_2S·2NaOH and Na_2S·NaOH. X-ray diffraction results obtained in this investigation for these two compositions along with Ovechkin et al. (*3*) data for Na_2S·2NaOH and literature data for Na_2S, NaOH, and Na_2S·$9H_2O$ are summarized in Table III. Our data for Na_2S·2NaOH and Na_2S·NaOH are quite satisfactorily accounted for on the basis of NaOH and Na_2S. Ovechkin et al. (*4*) data for Na_2S·2NaOH contain many additional lines. The most likely contaminants are H_2O and CO_2 or Na_2S·$9H_2O$ and Na_2CO_3. It is seen that most of the extra lines in Ovechkin's pattern can be accounted for on the basis of this hydrate, Na_2S, and NaOH. It is noted that the Na_2S lines tend to dominate these patterns particulary in the back-reflection region. In this region, all the patterns are in good agreement with the literature data for Na_2S. If compounds were formed, it would be very unlikely that these lines would correspond so closely to those for pure Na_2S and yield the same lattice constant.

Our data appear to show conclusively that these two compositions do not exist as distinct compounds but are merely mixtures of Na_2S and NaOH at room temperature.

NaOH–Na_2CO_3 System

Experimental data by Seward (*13*, *14*) and Khitrov (*15*), as summarized by Voskresenskaya (*10*), are plotted in Figure 3, Khitrov's data as solid points and Seward's data as open points. Not all of Seward's data were plotted for the NaOH-rich liquidus in order to show the liquidus curve. The melting temperature of NaOH, 319.2 °C, and the eutectic composition of 0.08 mole

Table III. X-ray Diffraction Data[a]

Ovechkin et al. $Na_2S·2NaOH$		diffraction data file							this investigation			
		23-441 Na_2S			1-1173 NaOH		18-1248 $Na_2S·9H_2O$		$Na_2S·NaOH$		$Na_2S·2NaOH$	
d, Å	I	d, Å	I/I_0	(hkl)	d, Å	I/I_0	d, Å	I/I_0	d, Å	I	d, Å	I
5.87	w				5.80	13	5.86	80	5.75	m	5.70	m
3.77	m	3.776	54	(111)			3.77	50	3.75	s	3.75	s
3.40	vw										3.35	vw
3.23	vw	3.269	4	(200)			3.21	90	3.27	m	3.25	vw
							3.11	40				
2.95	w						3.99	80	3.10	vvw		
2.83	w				2.85	20	2.80	100	2.85	ms	2.83	w
							2.64	60				
2.54	m						2.54	50	2.57	w		
2.46	vw						2.48	80				
2.40	vw						2.40	80				
					2.35	100			2.36	m	2.35	m
2.35	m	2.312	100	(220)					2.31	s	2.31	s
2.29	vw						2.30	40				
2.24	vw						2.24	40				
2.17	w						2.19	40	2.17	vvw		
2.13	w											
2.02	w				2.02	10			2.02	vw		
1.96	m	1.971	17	(311)			1.94	50	1.97	s	1.95	m
1.88	w	1.888	2	(222)	1.90	8			1.89	vw	1.89	vw
1.80	vw											
1.75	vw				1.70	30			1.70	w	1.69	vw
1.69	vw								1.65	w	1.65	vw
1.65	w	1.635	14	(400)	1.65	25			1.62	m	1.62	w
1.49	w	1.500	7	(331)					1.51	m	1.49	vw
1.47	vw	1.462	1	(420)	1.46	10			1.45	w	1.45	vvw
1.33	m	1.335	25	(422)	1.35	2			1.33	s	1.33	m
1.25	w	1.258	4	(511)	1.27	5			1.25	m	1.25	w
1.15	w	1.156	7	(440)	1.18	1			1.15	m	1.15	w
1.10	vw	1.105	5	(531)	1.10	m[b]			1.10	w	1.10	w
1.03	vw	1.034	10	(620)	1.03	vw			1.03	ms	1.03	w
0.995	vw	0.997	1	(553)					0.992	vw		
0.965	vw				0.958	ms			0.941	w	0.940	vvw
0.915	vw	0.916	2	(711)					0.912	vw	0.912	vvw
0.874	vw	0.874	7	(642)					0.872	m	0.872	m
0.850	vw	0.851	3	(731)					0.850	w	0.851	vw
									0.817	vw		
									0.799	vw		

[a] 1 nm = 10 Å; I/I_0 = relative intensities; I = visual intensities; v = very, s = strong, m = medium, w = weak. [b] Value from our powder pattern.

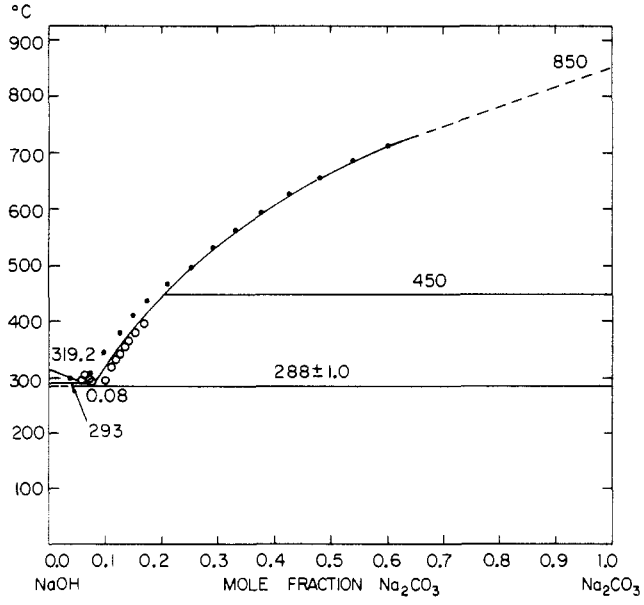

Figure 3. Binary Na_2CO_3–NaOH phase diagram. Seward (*13*, *14*) data are open points and Khitrov (*15*) data are closed points.

fraction NaOH, as determined by Morey and Burlew (*9*), were adopted. Their transition temperature of 293.1 °C is indicated as 293 °C in Figure 3. The melting temperature of 850 °C and a transition temperature of 450 °C for Na_2CO_3 are taken from the JANAF Tables (*8*).

Acknowledgment

Dale McMasters took the Debye–Scherrer diffraction patterns. Clifford Peterson conducted the chemical analysis on the dried Na_2S and NaOH. He also assisted in conducting some of the DTA experiments.

Registry No. Na_2S, 1313-82-2; NaOH, 1310-73-2; Na_2CO_3, 497-19-8.

Literature Cited

(1) Wheelock, T. D.; Markuszewski, R. In "The Science and Technology of Coal and Coal Utilization"; Cooper, B. R., Ellingson, W. A., Eds.; Plenum Press: New York, 1984; Chapter 3, pp 47–123.
(2) Chlotti, P.; Markuszewski, R., submitted to *Ind. Eng. Chem. Process Des. Dev.*
(3) Ovechkin, E. K.; Shevtsova, L. N.; Voltsekhovskii, A. E.; Obosnaya, L. I.; Kuznetsova, L. V. *Russ. J. Inorg. Chem.* (*Engl. Transl.*) **1973**, *18*, 571.
(4) Ovechkin, E. K.; Shevtsova, L. N. *Russ. J. Inorg. Chem.* (*Engl. Transl.*) **1974**, *18*, 1872.
(5) Kohlmeyer, E. J.; Lohrke, G. *Z. Anorg. Chem.* **1955**, *281*, 54.
(6) Steck, L.; Slavin, M.; Ralston, O. *J. Am. Chem. Soc.* **1929**, *51*, 3241.
(7) Kopylov, N. I.; Novoselov, S. S. *Russ. J. Inorg. Chem.* (*Engl. Transl.*) **1964**, *9*, 1038.
(8) Stull, D. R.; Prophet, H. "JANAF Thermochemical Tables", 2nd ed.; U.S. Government Printing Office: Washington, DC, 1971.
(9) Morey, G. W.; Burlew, J. S. *J. Phys. Chem.* **1964**, *68*, 1707.
(10) Voskresenskaya, N. K., Ed. "Handbook of Solid–Liquid Equilibria in Systems of Anhydrous Salts"; Izdatel'stvo Akademii Nauk SSSR: Moscow, 1961; Vol. 1 (English translation, U.S. DOE and NSF: Wash-

ington, DC; Israel Program for Scientific Translations, U.S. Department of Commerce, CFSTI: Springfield, VA, 1970).
(11) "Powder Diffraction File"; JCPDS, International Center for Diffraction Data: Swarthmore, PA 19081.
(12) Lee, T. S.; Chiotti, P.; Mason, J. T. *J. Less-Common Met.* **1979**, *66*, 33.
(13) Seward, R. P. *J. Am. Chem. Soc.* **1942**, *64*, 1053.
(14) Seward, R. P. *J. Am. Chem. Soc.* **1955**, *77*, 5507.
(15) Khitrov, V. A. *Izv. Sekt. Fiz.-Khim. Anal., Inst. Obshchel. Neorg. Khim., Akad. Nauk SSSR* **1954**, *25*, 236.

Received for review May 18, 1984. Accepted October 9, 1984. This work was supported by the Assistant Secretary for Fossil Energy, Division of Coal Utilization, through the Pittsburgh Energy Technology Center, Coal Preparation Branch.

Isothermal Vapor–Liquid Equilibria for the Ternary Methanol–Ethanol–Benzene System

Isamu Nagata

Department of Chemical Engineering, Kanazawa University, Kanazawa, Ishikawa 920, Japan

Vapor–liquid equilibrium data were measured for the methanol–ethanol–benzene system at 25 °C by using a Boublik vapor–liquid recirculation still. The results are correlated by the UNIQUAC and extended UNIQUAC models with binary parameters estimated from the maximum likelihood method.

In continuation of studies on isothermal vapor–liquid equilibria (VLE) for ternary alcohol mixtures, VLE data for the methanol–ethanol–benzene system at 25 °C are presented, because VLE data for ternary mixtures containing two alcohols are rarely available in the literature and VLE data for all three component binary systems at 25 °C have been published: methanol–ethanol (*1*), methanol–benzene (*2*), ethanol–benzene (*3*).

Experimental Section

All chemicals (first grade) were supplied by Wako Pure Chemical Industries, Ltd., and were purified. Alcohols were fractionally distilled in a 1-m column packed with McMahon packing after drying over drying materials: for methanol, anhydrous copper sulfate; and for ethanol, calcium oxide. Benzene was subjected to repeated recrystallization. Densities, measured with an Anton Paar DMA40 densimeter, and vapor pressures of these compounds at 25 °C are compared with literature values as shown in Table I.

The still used to obtain VLE data for the ternary system was a Boublik vapor–liquid recirculation still (*3*). This still has some advantages as follows: relatively easy operation at 25 °C, high accuracy at low pressure, and no stopcock in contact with sample liquids. Figure 1 shows the all-glass equilibrium still with modifications. An internal platinum heater was inserted into the boiling flask in order to boil the liquid smoothly, and mixing within the liquid sample tubes was performed by magnetic stirrers. A copper–constantan thermocouple calibrated against a Hewlett-Packard 2804A standard quartz thermometer and a Yokogawa P-7B potentiometer connected to a galvanometer were used to measure the equilibrium temperature. The equilibrium pressures were measured by using a mercury manometer and a cathetometer and then corrected to give the equivalent height of a mercury column at 0 °C and standard gravity. The still was loaded with about 80 cm^3 of mixture. The pressure in the still was adjusted until a temperature of 25 °C in the equilibrium was maintained. Liquid samples of two phases in equilibrium were obtained when each experimental run had continued at 25 °C for 2–3 h.

The compositions of the obtained liquid and condensated vapor samples were determined by using a Shimadzu GC-7A gas chromatograph equiped with a Shimadzu ITG-2A digital integrator. The observed values were estimated to have the following experimental errors: pressure, 13 Pa; composition, 0.002 mole fraction; temperature, 0.05 K.

Table I. Densities and Vapor Pressures of Components at 25 °C

	density, g cm^{-3}		vapor press., kPa	
compd	this work	lit. (*4*)	this work	lit. (*4*)
methanol	0.7866	0.786 64	16.692	16.669
ethanol	0.7850	0.785 04	7.973	7.969
benzene	0.8737	0.873 70	12.772	12.692

Experimental Results and Correlations

Experimental vapor–liquid equilibrium data are given in Table II with values of activity coefficients calculated from the relation

$$\gamma_i = \phi_i y_i P / \{\phi_i^s x_i P_i^s \exp[v_i^L (P - P_i^s)/RT]\} \quad (1)$$

where the fugacity coefficients, ϕ_i and ϕ_i^s, were calculated by using the volume-explicit virial equation truncated after the second term and second virial coefficients estimated from the Hayden and O'Connell method (*5*). The virial coefficients are reported in Table II. The liquid molar volumes v_i^L were calculated from the modified Rackett equation (*6*).

The ternary VLE data were correlated with the UNIQUAC and extended UNIQUAC activity coefficient models (*7*, *8*). The UNIQUAC model gives the activity coefficient for any component i in a multicomponent mixture by

$$\ln \gamma_i = \ln (\Phi_i/x_i) + 1 - \Phi_i/x_i - (Z/2) q_i \{\ln (\Phi_i/\theta_i) + 1 - \Phi_i/\theta_i\} - q_i' \ln (\sum_j \theta_j' \tau_{ji}) + q_i' - q_i' \sum_j \frac{\theta_j' \tau_{ij}}{\sum_k \theta_k' \tau_{kj}} \quad (2)$$

where Z is the coordination number equal to 10, and the segment fraction Φ, the area fractions θ and θ', and an adjustable parameter τ_{ij} are given by

$$\Phi_i = r_i x_i / \sum_j r_j x_j \quad (3)$$

$$\theta_i = q_i x_i / \sum_j q_j x_j \quad (4)$$

$$\theta_i' = q_i' x_i / \sum_j q_j' x_j \quad (5)$$

$$\tau_{ij} = \exp(-a_{ij}/T) \quad (6)$$

The pure-component structural parameters for each component are as follows: for methanol, $r = 1.43$, $q = 1.43$, $q' = 0.96$; for ethanol, $r = 2.11$, $q = 1.97$, $q' = 0.92$; and for benzene,

0021-9568/85/1730-0201$01.50/0